

2009

## **Nuclear Forces and High-Performance Computing: The Perfect Match**

T. Luu

A. Walker-Loud  
*William & Mary*

Follow this and additional works at: <https://scholarworks.wm.edu/aspubs>

---

### **Recommended Citation**

Luu, T., & Walker-Loud, A. (2009). Nuclear forces and high-performance computing: The perfect match. In *Journal of Physics: Conference Series* (Vol. 180, No. 1, p. 012081). IOP Publishing.

This Article is brought to you for free and open access by the Arts and Sciences at W&M ScholarWorks. It has been accepted for inclusion in Arts & Sciences Articles by an authorized administrator of W&M ScholarWorks. For more information, please contact [scholarworks@wm.edu](mailto:scholarworks@wm.edu).

# Nuclear Forces and High-Performance Computing: The Perfect Match

T Luu<sup>1</sup>, A Walker-Loud<sup>2</sup>

<sup>1</sup> N-division, Lawrence Livermore National Laboratory, Livermore, CA 94551 USA

<sup>2</sup> Physics Department, College of William and Mary, Williamsburg, VA 23187-8795 USA

E-mail: tluu@llnl.gov

**Abstract.** High-performance computing is now enabling the calculation of certain hadronic interaction parameters directly from Quantum Chromodynamics, the quantum field theory that governs the behavior of quarks and gluons and is ultimately responsible for the nuclear strong force. In this paper we briefly describe the state of the field and show how other aspects of hadronic interactions will be ascertained in the near future. We give estimates of computational requirements needed to obtain these goals, and outline a procedure for incorporating these results into the broader nuclear physics community.

## 1. Introduction

High-performance computing is fast becoming an integral part of nuclear physics, acting as a third pillar of scientific research standing next to theory and experiment. This integration has brought with it a new understanding of how certain aspects of hadronic (nuclear) forces comes from Quantum Chromodynamics (QCD), the field theory that describes the interactions of a set of nature's fundamental particles, quarks and gluons.

Lattice QCD (LQCD), the numerical implementation of QCD on a discretized space-time lattice, is now emerging as a powerful calculational tool of nuclear physics observables. Even at this early stage, the results are impacting the broader nuclear physics community. With ever increasing high-performance computing, longstanding nuclear physics questions, such as the nature of the nuclear spin-orbit coupling and the three-body interaction, will be tackled directly by LQCD. Further, the predictive capability of LQCD will allow scientists to understand nuclear phenomena in extreme environments not accessible by experiment like those found in the birth and death throes of a star or in the crusts of neutron stars.

Current computer limitations have restricted lattice QCD calculations to a regime where the light quark masses are equal (isospin limit) and unnaturally large. This equates to pion masses  $m_\pi$  typically  $\geq 300$  MeV.<sup>1</sup> Even though this does not represent the physical world, calculations in this regime have resulted in a deeper understanding of nuclear physics. We highlight a few examples below. These examples are by no means exhaustive.

<sup>1</sup> With the ever increasing high-performance computing capabilities, this scenario is rapidly changing. Within the last year lattice gauge configurations have been generated with  $m_\pi \simeq 190$  MeV.

### 1.1. Nuclear physics is perturbative at large $m_\pi$

The study of hadron interactions with lattice QCD is different from scattering experiments in a conceptually important way; lattice calculations are limited to probing multi-particle interactions with a finite, Euclidean volume. Therefore, the particles can not be asymptotically separated from each other, nor can the in/out states be brought onto their mass shell. Consequently, one can not perform “scattering experiments” with lattice calculations, except at kinematic thresholds, since Euclidean Green’s functions are not simply related to the physical  $S$ -matrix elements [1]. However, it has been shown that the energy levels of particles in a finite volume can be related to the infinite volume scattering parameters [2], and in particular for two particles to the scattering phase shift. This formalism was extended by Lüscher to interacting relativistic field theories [3, 4], with the degenerate, two-particle phase shift given by

$$\frac{p \cot \delta(p)}{m} = \frac{1}{\pi m L} S \left( \frac{pL}{2\pi} \right), \quad (1)$$

where  $S(x)$  is a known function dependent upon the geometry of the spatial volume and the interaction momenta is defined by

$$\Delta E_{HH} \equiv E_{HH} - 2m = 2\sqrt{p^2 + m^2} - 2m, \quad (2)$$

and  $\delta(p)$  is the infinite volume scattering phase shift<sup>2</sup> and  $m$  is the mass of either particle. For low momentum interactions, one has

$$\frac{p \cot \delta(p)}{m} = -\frac{1}{ma} + \frac{1}{2}(mr) \left( \frac{p}{m} \right)^2 + \dots \quad (3)$$

where  $a$  is the scattering length,  $r$  is the effective range and the ellipses denote further suppressed terms in the effective-range expansion. It is important to note the range of validity of this formalism, which has come to be known as Lüscher’s method. Equation (1) is only valid below the inelastic threshold. Further, it has been assumed the effective range of the interaction is much smaller than the spatial volume,  $r \ll L$ . However, there are no restrictions on the scattering length, which is important for nuclear physics, since at the physical pion mass, we know the  $^1S_0$  and  $^3S_1$  scattering lengths are unnaturally large, with  $a(^1S_0) \simeq -23.7$  fm and  $a(^3S_1) \simeq 5.4$  fm, while typical lattice calculations today have  $L \simeq 2.5$ – $3$  fm. For  $a \ll L$ , the interaction energy can be expressed as

$$\Delta E = \frac{4\pi a}{mL^3} - \frac{4a^2}{mL^4} \mathcal{I} + \frac{4a^3}{\pi^2 mL^5} [\mathcal{I}^2 - \mathcal{J}] + O(L^{-6}) \quad (4)$$

where  $\mathcal{I}$  and  $\mathcal{J}$  are known geometrical constants whose numerical values are given in tab. 1 for a square, periodic spatial volume. The relation in the converse limit,  $a \gg L$ , relevant for  $NN$  interactions near the physical point was derived in Ref. [10].

The first dynamical calculation of nucleon-nucleon scattering with lattice QCD was only recently carried out at three values of the pion mass with  $m_\pi \geq 350$  MeV [11]. It was found that at these pion masses, the interaction was weakly repulsive in both the  $^1S_0$  and  $^3S_1$  channels, see Fig. 1. This is in contrast to the same system at the physical pion mass, where we know that, for example, the deuteron is (weakly) bound and has an unnaturally large scattering length,  $a/r \gg 1$ . *Nature’s fine tuning of the NN system disappears for large  $m_\pi$ .*

<sup>2</sup> It has been asserted in the literature that lattice QCD can be used to directly calculate the nuclear potential [5, 6]. However, as pointed out in [7, 8, 9], this assertion is false since in an interacting field theory, like QCD, except for infinitely heavy particles, there is no unique definition of a potential as it is not an observable quantity. The only things which can be rigorously computed are n-point Green’s functions, which can then be related to infinite volume scattering parameters.

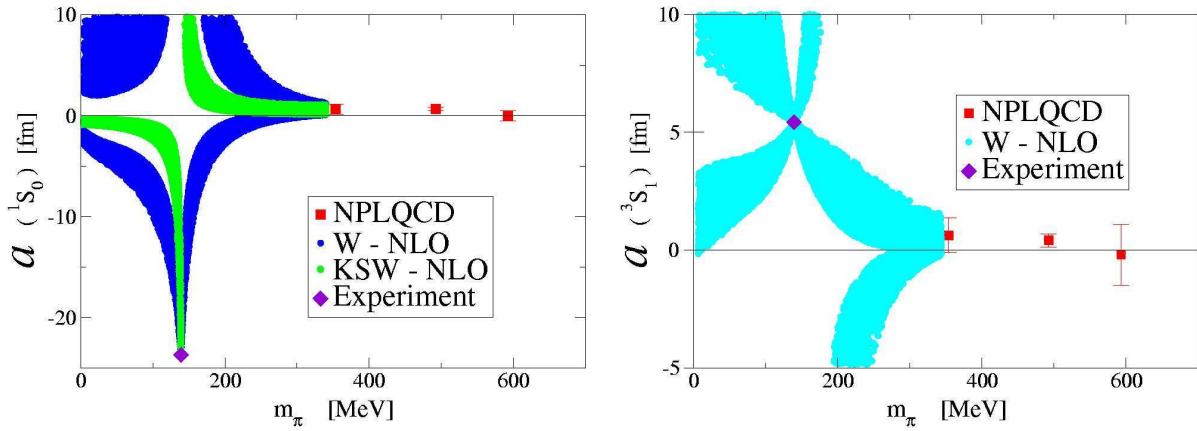


**Figure 1.** NPLQCD calculation of NN scattering lengths [11].

Beane et al.'s results suggest that standard perturbation theory applies to hadronic systems in the large  $m_\pi$  regime. We can parametrize the interaction between hadrons by partial waves using short-ranged repulsive forces that have interaction terms of 'natural size',

$$V_0(\vec{p}', \vec{p}) = \frac{4\pi a_0}{m} \left[ 1 + \frac{a_0 r_0}{2} \left( \frac{p'^2 + p^2}{2} \right) + \dots \right] \quad (\text{s-wave}) \quad (5)$$

$$V_1(\vec{p}', \vec{p}) = \frac{12\pi a_1}{m} \vec{p}' \cdot \vec{p} \left[ 1 + \frac{a_1 r_1}{2} \left( \frac{p'^2 + p^2}{2} \right) + \dots \right] \quad (\text{p-wave}) \quad (6)$$

$$V_2(\vec{p}', \vec{p}) = \frac{10\pi a_2}{m} (3(\vec{p}' \cdot \vec{p})^2 - p'^2 p^2) \left[ 1 + \frac{a_2 r_2}{2} \left( \frac{p'^2 + p^2}{2} \right) + \dots \right] \quad (\text{d-wave}), \quad (7)$$

and so on. The parameters  $a_l$  and  $r_l$  constitute part of the effective range parameters from scattering theory. Depending on the partial wave, these parameters have different dimensions. Perturbation theory remains valid as long as  $a_0/L \ll 1$  and  $r_0/L \ll 1$ , as well as  $a_1/L^3 \ll 1$  and  $r_1 L \ll 1$ , and so forth.

In most of the sections below we assume that perturbation theory holds for hadronic systems, since to date LQCD calculations are still in a regime where  $m_\pi$  is large. In sect. 4 we briefly outline the methods needed to go beyond perturbation theory.

### 1.2. Weinberg's leading order prediction works very well for mesons

The simplest system of interacting hadrons, both theoretically and numerically is that of two pions in the isospin  $I = 2$  channel.<sup>3</sup> The simplicity of this system follows from the fact that the pions are the pseudo-Goldstone bosons associated with the spontaneous breaking of the approximate chiral symmetry of QCD. At leading order (LO) in chiral perturbation theory ( $\chi$ -PT), the  $\pi\pi$  interactions are uniquely predicted, first determined by Weinberg in 1966 [12], with the scattering lengths given by

$$m_\pi a_{\pi\pi}^{I=0} = -\frac{7m_\pi^2}{16\pi f_\pi^2}, \quad m_\pi a_{\pi\pi}^{I=2} = \frac{m_\pi^2}{8\pi f_\pi^2}. \quad (8)$$

Subleading orders in the chiral expansion give rise to perturbatively small corrections containing both non-analytic contributions as well as analytic terms whose coefficients are not determined

<sup>3</sup> The  $I = 0$  channel is complicated by the presence of the scalar resonance,  $\sigma$ . Additionally, numerical computations of scalar scattering channels are complicated by the necessity of including the numerically-expensive disconnected quark propagators.

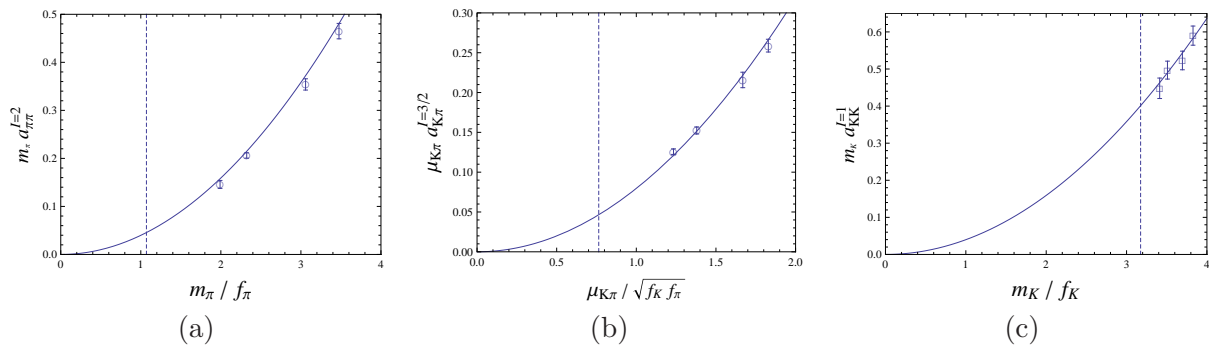


**Figure 2.** NPLQCD calculated values of the  $I = 2$   $\pi\pi$  (a),  $I = 3/2$   $K\pi$  (b) and  $I = 1$   $KK$  (c) scattering lengths. In all cases, the numerical-data are plotted vs. the lattice-physical masses and decay constants, as calculated for each ensemble. The dashed lines represent the physical point and the curves are Weinberg's LO prediction. The reduced mass is  $\mu_{K\pi} = m_K m_\pi / (m_K + m_\pi)$ . The LO predictions for the  $K\pi$  and  $KK$  system at the physical pion mass are  $m_K a_{KK}^{I=1} = \frac{m_K^2}{8\pi f_K^2}$  and  $\mu_{K\pi} a_{K\pi}^{I=3/2} = \frac{\mu_{K\pi}^2}{4\pi f_\pi f_K}$ .

**Table 1.** Numerical values of geometrical sums appearing in this document.

$\mathcal{I}$	$\mathcal{J}$	$\mathcal{K}$	$\mathcal{L}$	$\mathcal{M}$
-8.9136	16.5323	8.4019	-6.3748	18.3

by chiral symmetry alone [13]. These coefficients must be determined either with a comparison to experiment or to numerical results from lattice QCD.

In 2005, the NPLQCD Collaboration performed the first lattice calculation of  $I = 2$   $\pi\pi$  scattering containing both light and strange dynamical quarks [14]. Because the low energy pion interactions are strongly constrained by chiral symmetry, the lattice calculation was performed with a mixed action using domain-wall valence quarks [15, 16, 17] (which retain a lattice chiral symmetry), with the `asqtad` improved [18, 19] staggered MILC gauge ensembles [20]. In 2007, the calculation was updated with a significant increase in statistics, as well as the use of the relevant mixed action  $\chi$ -PT expression to perform the extrapolation to the physical point [21, 22, 23, 24, 25, 26, 27]. The result was a 1% prediction (including systematic errors) of the  $I = 2$   $\pi\pi$  scattering length, expressed at the value of the charged pion mass [28],

$$m_\pi a_{\pi\pi}^{I=2} = 0.04330 \pm 0.00042, \quad (9)$$

a value competitive with the best theoretical predictions [29, 30]. *The precision of these LQCD measurements surpasses that of experiment.*

With the same mixed action, the NPLQCD Collaboration has similarly computed the values of the  $I = 3/2$   $K\pi$  [31] and  $I = 1$   $KK$  [32] scattering lengths as well as  $f_K/f_\pi$  [33]. The high precision attained in the lattice calculation of these quantities, combined with the  $I = 2$   $\pi\pi$  results, can be used to provide stringent checks of low energy dynamics predicted by  $SU(2)$  and  $SU(3)$   $\chi$ -PT.

One interesting phenomenon which has been observed is that the scattering lengths, for all values of the light and strange quark masses used, are remarkably well described by the LO predictions of Weinberg, see Fig.2, for which there is presently no theoretical understanding.

### 1.3. Lattice QCD can probe systems that are not accessible experimentally

The most powerful aspect of LQCD is its predictive capability. With sufficient computer resources, systems not accessible by experiment can be calculated on a lattice. In most cases, these systems have impact in many areas of nuclear physics, such as nuclear astrophysics. A recent example of this predictive capability came from LQCD simulations of multiple pions and kaons in a box. Because of chiral symmetry, the perturbative nature of these systems is well established and general finite-volume formulas can be derived that relate the ground state interacting energies of these systems (measured by LQCD) to interaction parameters as a function of the number of mesons  $n$  [34, 35],

$$E_{A_1}(n) = \frac{4\pi a_0}{mL^3} \binom{n}{2} \left\{ 1 - \frac{a_0 \mathcal{I}}{\pi L} + \left( \frac{a_0}{\pi L} \right)^2 [\mathcal{I}^2 + (2n - 5)\mathcal{J}] - \left( \frac{a_0}{\pi L} \right)^3 [\mathcal{I}^3 + (2n - 7)\mathcal{I}\mathcal{J} + (5n^2 - 41n + 63)\mathcal{K}] \right\} + \binom{n}{2} \frac{8\pi^2 a_0^2 r_0}{mL^6} + \binom{n}{3} \frac{\eta_3}{L^6} + O(L^{-7}). \quad (10)$$

At order  $1/L^6$ , a dressed pure three-body interaction is needed to enforce cutoff independence. Detmold et al. used LQCD-measured interaction energies of different numbers of pions [36, 37] to extract this force, finding that it is repulsive with a size consistent with naive dimensional analysis. A subsequent work determined the equivalent three body interaction for charged kaons [38] finding an interaction strength consistent with zero. *For the first time, LQCD is allowing definitive statements of hadronic three-body forces to be made.*

### 1.4. Three Baryon States with lattice QCD

Recently a high-statistics exploration of a three-baryon signal with the same quantum numbers of the  $\Xi^0 \Xi^0 n$  system was undertaken, finding on a single ensemble with  $m_\pi \simeq 390$  MeV,  $E_{\Xi\Xi N} = 3877.9 \pm 6.9 \pm 9.2 \pm 3.3$  MeV, where the first uncertainty is statistical and the second and third uncertainties are estimates of fitting systematics [39]. Despite the remarkable level of precision in this calculation, no extraction of interaction parameters was performed. Lattice QCD calculations of multi-baryon systems are emblematic of the stochastic nature of these simulations, suffering poorer signal-to-noise ratios compared to their mesonic counterparts. Extracting a pure three-baryon interaction will require sufficiently more computational resources than available today, as well as improved algorithms. In Refs. [39, 40], the NPLQCD Collaboration undertook a significant, high-statistics scaling study of the extraction of (multi) baryon energy levels from lattice QCD calculations. This provides the basis for our resource estimates required for these types of calculations in sect. 5.

## 2. Going beyond $A_1$ (s-wave) cubic symmetry

Lattice calculations typically involve simulations inside a periodic box. System wavefunctions with angular momentum for integer and odd-half states are therefore characterized by the irreducible representations (irreps) of the cubic (octahedral) group  $O$  and its cover,  $O_h$ , respectively. For zero center of mass (CM) systems, integer (spatial) states fall into one of five representations:  $A_1$ ,  $A_2$ ,  $T_1$ ,  $T_2$ , and  $E$ . Odd-half states belong to either  $G_1$ ,  $G_2$ , or  $H$  representations. There is extensive literature on how these states are comprised of infinite-volume, continuum angular momentum states of  $SO(3)$  (e.g. [41]). For example, ground-state  $A_1$  systems represent s-wave systems in the infinite-volume limit, whereas ground-state  $T_1$  systems represent p-wave systems in this limit.

To date all calculations have been on systems with spatial  $A_1$  symmetry. Projection onto this symmetry is simplest, as it represents the most ‘symmetric’ and least time-consuming operation.

With future high-performance computing, and the need to look beyond two-baryon systems, other cubic symmetries will be probed, giving new information about the interaction between hadrons.

For example, with two identical baryons, projection onto the negative parity  $T_1$  spatial symmetry will force ground-states to be perturbatively connected to the non-interacting state with kinetic energy  $4\pi^2/mL^2$ , or the first cubic shell. The simplest system to consider consists of a neutron and proton with spatial  $T_1$  and spin  $A_1$  coupled to total angular momentum  $T_1$ , *i.e.*  $|(T_{1u}A_1)T_{1u}\rangle$ . The energy of this system to order  $1/L^5$  is

$$E_{(T_{1u}A_1)T_{1u}} = \frac{4\pi^2}{mL^2} + \frac{96\pi^3 a_1}{mL^5} + O(L^{-7}) . \quad (11)$$

Beyond the kinetic energy term,  $4\pi^2/mL^2$ , the leading order term of this system is only sensitive to the “scattering volume”,  $a_1$ . In the infinite volume, continuum limit this state maps to the  ${}^1P_1$  scattering state.

At  $1/L^5$  we can also extract information about non-central forces by looking at, for example, two neutrons with spatial  $T_1$  symmetry coupled to spin  $T_1$  symmetry. In the infinite volume limit, this system can belong to three possible scattering states:  ${}^3P_0$ ,  ${}^3P_1$ , and  ${}^3P_2$ . In a box, these states are split up into four possibilities,  $|(T_{1u}T_1)A_{1u}\rangle$ ,  $|(T_{1u}T_1)T_{1u}\rangle$ ,  $|(T_{1u}T_1)T_{2u}\rangle$ , and  $|(T_{1u}T_1)E_u\rangle$ . If life consisted of only central forces these states would be degenerate. Non-central forces, on the other hand, will break this degeneracy. The strength and order of the broken degeneracies give us information about the nature of the non-central force. For example, if we identify a source of the non-central force as coming from virtual one-pion exchange (OPE),

$$V_\pi(\vec{q}) = - \left( \frac{g_A}{\sqrt{2}f_\pi} \right)^2 (\tau_1 \cdot \tau_2) \frac{(\vec{\sigma}_1 \cdot \vec{q})(\vec{\sigma}_2 \cdot \vec{q})}{q^2 + m_\pi^2} , \quad (12)$$

where  $\vec{q}$  is the momentum transfer carried by the virtual pion,  $g_A$  is the axial-vector coupling, and  $f_\pi$  is the pion decay constant, we find that the degeneracies are broken in the following manner:

$$E_{(T_{1u}T_1)A_{1u}} = \frac{4\pi^2}{mL^2} + \frac{96\pi^3 a_1}{mL^5} + \frac{8\pi^2 g_A^2}{3f_\pi^2 m_\pi^2 L^5} - \frac{80\pi^2 g_A^2}{3f_\pi^2 m_\pi^2 L^5} + O(L^{-7}) \quad (13)$$

$$E_{(T_{1u}T_1)T_{1u}} = \frac{4\pi^2}{mL^2} + \frac{96\pi^3 a_1}{mL^5} + \frac{8\pi^2 g_A^2}{3f_\pi^2 m_\pi^2 L^5} + \frac{40\pi^2 g_A^2}{3f_\pi^2 m_\pi^2 L^5} + O(L^{-7}) \quad (14)$$

$$E_{(T_{1u}T_1)T_{2u}} = \frac{4\pi^2}{mL^2} + \frac{96\pi^3 a_1}{mL^5} + \frac{8\pi^2 g_A^2}{3f_\pi^2 m_\pi^2 L^5} + O(L^{-7}) \quad (15)$$

$$E_{(T_{1u}T_1)E_u} = \frac{4\pi^2}{mL^2} + \frac{96\pi^3 a_1}{mL^5} + \frac{8\pi^2 g_A^2}{3f_\pi^2 m_\pi^2 L^5} + O(L^{-7}) , \quad (16)$$

where the terms in red (blue) come from the central (non-central) part of OPE. At this order, the scattering volume can be re-defined to absorb the central part of OPE,  $a_1 \rightarrow a_1 + \frac{g_A^2 m}{36\pi f_\pi^2 m_\pi^2}$ <sup>4</sup>. But the non-central parts clearly break the degeneracy for the  $|(T_{1u}T_1)A_{1u}\rangle$  and  $|(T_{1u}T_1)T_{1u}\rangle$  states. LQCD calculations of these energies will therefore tell us of the existence and strength of the tensor interaction.

Interaction terms of higher partial waves can be probed with appropriate projections onto other spatial symmetry groups. For example, the infinite volume  ${}^1D_2$  scattering state will have

<sup>4</sup> The central part of OPE also contributes at order  $1/L^5$  in eq.(11) but can be absorbed into the scattering volume with the following re-definition:  $a_1 \rightarrow a_1 + \frac{g_A^2 m}{4\pi f_\pi^2 m_\pi^2}$ .



the following ground state energy in a box,

$$E_{(E_g A_1) E_g} = \frac{4\pi^2}{mL^2} + \frac{240\pi^5 a_2}{mL^7} + O(L^{-8}). \quad (17)$$

In general higher partial wave interaction terms will be suppressed by larger powers of  $L$ , and because of the finite dimensionality of the cubic group, operator mixing between different partial waves will occur.

Similar results can be obtained in three-baryon systems. In [42] perturbative results were given for a three-neutron system. Here we concentrate on the ‘‘perturbative’’ triton system whose energy is

$$E_{(A_{1g} G_1) G_{1g}} = 0 + \frac{12\pi}{mL^3} \left( \frac{a_0^s + a_0^t}{2} \right) - \frac{12}{mL^4} \left( \frac{(a_0^s)^2 + (a_0^t)^2}{2} \right) \mathcal{I} \\ + \frac{12}{\pi mL^5} \left( \frac{(a_0^s)^3 + (a_0^t)^3}{2} \right) \mathcal{I}^2 + \frac{12}{\pi mL^5} \left( \frac{a_0^s + a_0^t}{2} \right) [(a_0^s)^2 + (a_0^t)^2] \mathcal{J} + O(L^{-6}). \quad (18)$$

Here  $a_0^s$  and  $a_0^t$  are the scattering lengths for the spin-singlet and spin-triplet channels, respectively. The negative parity triton has two states that are perturbatively connected to the first cubic shell,

$$E_{(T_{1u} G_1) G_{1u}} = \frac{4\pi^2}{mL^2} + \frac{12\pi}{mL^3} \left( \frac{a_0^s + a_0^t}{2} \right) - \frac{12}{mL^4} \left( \frac{(a_0^s)^2 + (a_0^t)^2}{2} \right) \left[ \mathcal{L} + \frac{1}{4} \right] + \frac{9a_0^s a_0^t}{mL^4} \\ + \frac{12}{\pi mL^5} \left( \frac{(a_0^s)^3 + (a_0^t)^3}{2} \right) \left[ \mathcal{L}^2 + \frac{1}{2} (\mathcal{L} - \mathcal{M}) - \frac{1}{16} \right] - \frac{(a_0^s)^2 a_0^t + (a_0^t)^2 a_0^s}{\pi mL^5} \left[ 9\mathcal{L} + 3\mathcal{M} - \frac{15}{8} \right] \\ + \frac{6\pi^3}{mL^5} \left( \frac{(a_0^s)^2 r_0^s + (a_0^t)^2 r_0^t}{2} \right) + \frac{108\pi^3}{mL^5} \left( \frac{a_1^s + a_1^t}{2} \right) + O(L^{-6}), \quad (19)$$

and

$$E_{(T_{1u} G_1) H_{1u}} = \frac{4\pi^2}{mL^2} + \frac{144\pi^3}{mL^5} \left( \frac{a_1^s + a_1^t}{2} \right) + O(L^{-6}). \quad (20)$$

$r_0^s$  ( $a_1^s$ ) and  $r_0^t$  ( $a_1^t$ ) are the effective ranges (scattering volumes) in the spin-singlet and spin-triplet channels, respectively. In the infinite volume limit these states correspond to  $|J^\pi \rangle = |\frac{1}{2}^- \rangle$  and  $|\frac{3}{2}^- \rangle$ .

### 3. LQCD offers an ideal place for performing nuclear physics ‘‘experiments’’

Though not utilized to date, LQCD calculations of nuclear systems can be performed with non-zero CM motion. Because of the box boundary conditions, one can take advantage of this option to further probe aspects of hadronic interactions. Angular momentum states are not part of the full cubic group, however, as only cubic operations that preserve the CM momentum vector are allowed. As such, the classification of angular momentum states falls into subgroups, or little groups, of the cubic group [43, 44]. A consequence of this is that the mapping of infinite volume angular momentum states to point-group irreps can be different for non-zero CM. For example, ground state p-wave systems can be part of the  $A_1$  symmetry for states with non-zero CM, as opposed to  $T_1$  symmetry for zero CM.

For two baryons, the simplest way to enforce non-zero CM motion is to give one of the baryons the smallest momentum allowed by the box,  $2\pi/L$ . Angular momentum states must fall into the irreps of the  $C_{4v}$  group. For example, two neutrons with spins oppositely aligned have their ground state energy as

$$E_{A_1} = \frac{2\pi^2}{mL^2} + \frac{8\pi a_0}{mL^3} - \frac{8a_0^2}{mL^4} \mathcal{L} + \frac{8a_0^3}{\pi mL^5} [\mathcal{L}^2 - \mathcal{M}] + \frac{4\pi^3 a_0^2 r_0}{mL^5} + O(L^{-6}). \quad (21)$$



Compare this to the same energy with zero CM motion given in eq.(4). Because eq.(21) is not perturbatively connected to zero, but to  $2\pi^2/mL^2$ , expressions involving the effective range are not derivatively suppressed and show up at  $1/L^5$ .

On the other hand, if the two neutrons have their spins aligned their ground state energy is

$$E_{A_1} = \frac{2\pi^2}{mL^2} + \frac{24\pi^3 a_1}{mL^5} + O(L^{-6}) . \quad (22)$$

In this case the energy shift is sensitive to  $a_1$ . This system also belongs to the  $A_1$  irrep of  $C_{4v}$ , even though it would correspond to a p-wave system in the infinite volume limit. Further, it is perturbatively connected to  $2\pi^2/mL^2$ , as is eq.(21). One does not have to go to a higher cubic shell to probe the scattering volume, as was done in the previous section; one need only project onto the correct spin state.

In addition to working with non-zero CM motion, calculations can also be done on lattices with asymmetric spatial volumes. Angular momentum states, in this case, will also be restricted to subgroups of  $O$  in a similar (but not exact) manner as the examples above. This gives another handle on probing various aspects of the interaction between hadrons. In this sense, LQCD offers a unique and powerful “experimental” platform for learning the nature of hadronic forces.

#### 4. As $m_\pi \rightarrow 140$ MeV, life *will* become non-perturbative

Self-bound, non-perturbative states of multi-nucleons exist in nature (i.e. nuclei). As lattice calculations approach the physical pion mass these states are expected to form and the perturbative expressions of the previous sections will become inadequate. Fortunately for the two nucleon case eq. (1) still holds. In principle, EFT prescriptions for constructing potentials from these results can be used, giving (schematically)

$$V_0(\vec{p}', \vec{p}) = f_0^R(p'^2, p^2) \quad (\text{s-wave}) \quad (23)$$

$$V_1(\vec{p}', \vec{p}) = (\vec{p}' \cdot \vec{p}) f_1^R(p'^2, p^2) \quad (\text{p-wave}) \quad (24)$$

$$V_2(\vec{p}', \vec{p}) = (3(\vec{p}' \cdot \vec{p})^2 - p'^2 p^2) f_2^R(p'^2, p^2) \quad (\text{d-wave}) , \quad (25)$$

and so on. Here  $f_i^R$ , being functions of only the magnitude of the initial and final momenta, are chosen to reproduce, among other things, the effective range parameters. The superscript  $R$  refers to the particular regularization scheme employed.

For three-baryon systems there is no analogue of eq. (1). Recently there has been work on understanding the three-fermion system at the unitary limit ( $a_0 \rightarrow \infty$ ) within a box [45], as well as three-bosons [46], but a general non-perturbative method utilizing box-boundary conditions that includes other interaction terms has not been developed. Here we outline a method that solves the secular equation,

$$H_{eff}(E)P|\Psi \rangle = \left\{ H + V \frac{1}{E - QH} QV \right\} P|\Psi \rangle = E P|\Psi \rangle , \quad (26)$$

using Faddeev techniques. The term  $V$  represents the interaction between baryons (*e.g.* Eqs.(23)-(25)) which can include a pure three-baryon term. The projection operators  $Q$  and  $P$  are chosen such that  $Q + P = 1$  and they commute with the kinetic energy operator,  $[Q, T] = [P, T] = 0$ . The state  $|\Psi \rangle$  represents the (as yet unknown) eigenstate of the interacting three-body system and  $E$  represents the exact (to be determined) eigenvalue. The effective Hamiltonian is only applicable in the ‘model’ space defined by  $P$  and is energy-dependent. The space defined by  $P$  usually represents the lowest modes of the system, and in this case, will be defined by non-interacting, fully anti-symmetric states of definite cubic symmetry that reside in the first few cubic shells of the box.

As described in [47], part of eq.(26) can be recast into integral form by using Faddeev decompositions,

$$|\psi_i \rangle = \mathcal{T}^Q |\Omega_i \rangle + \mathcal{T}^Q G_0(E) \Pi |\psi_i \rangle, \quad (27)$$

where  $\Pi = 1 + P_{12}P_{13} + P_{12}P_{23}$  is a sum of permutation operators,  $G_0(E) = 1/(E - T)$  is the non-interacting three-body propagator, and

$$\mathcal{T}^Q = V + V G_0(E) Q \mathcal{T}^Q \quad (28)$$

is the ‘excluded-space’ T-matrix. The state  $|\Omega_i \rangle$  resides in the model space, *i.e.*  $|\Omega_i \rangle \in P$ , and  $|\psi_i \rangle$  must be numerically determined. There are standard techniques for solving the integral equation in eq.(27).

Given  $|\psi_i \rangle$ , model space matrix elements of  $H_{eff}$  are related by

$$\langle \Omega_j | H_{eff}(E) | \Omega_i \rangle = \langle \Omega_j | T | \Omega_i \rangle + \langle \Omega_j | \psi_i \rangle. \quad (29)$$

As the energy  $E$  is not known *a priori* (it is what we are trying to determine), in practice a starting guess for  $E$  is used to construct these matrix elements, which in turn are diagonalized to obtain a new  $E$ . This value is used to construct new matrix elements, which are then diagonalized, and so on. The process repeats itself until the input energy is the same as the energy after diagonalization. In [42] we describe how to construct the non-interacting, anti-symmetric states  $|\Omega_i \rangle$ . This procedure has been applied to self-bound nucleons in the infinite volume limit [47] and to fermions bound in an optical trap [48]

Having a non-perturbative, three-baryon formalism with box-boundary conditions is an essential step for extracting any pure three-baryon force. In a similar fashion described in sect. 1.3, information about the 4-, 5-, and higher-baryon systems can be used to also extract the three-baryon force, but due to complexities inherent to baryon systems this procedure will be tedious and require enormous computing resources. On the other hand, one can investigate the three-baryon system (including its excited states) using non-zero CM motion, or within asymmetric spatial volumes, in an analogous manner described in the previous sections. These systems will also give insight into the three-baryon force.

## 5. What does it take to get there?

The work described in sects. 1.1–1.4 resulted from teraflop-sized calculations using lattice gauge ensembles with large pion masses ( $m_\pi > 290$  MeV), relatively course lattice spacings ( $a \sim 0.1$  fm), and limited spatial volumes ( $L = 3.5 \sim 4$  fm). Ensembles at the physical pion mass, using fine lattice spacings  $a < 0.1$  fm, and within large volumes  $L > 7$  fm will require full petaflop resources or more. Further, measurements performed on these ensembles that are relevant to nuclear physics will require commensurate resources. Extraction of interaction parameters within two-baryon systems at a precision that competes with experiment will also require dedicated petaflop resources (at least). In the meson sector requirements are less restrictive. The superior signal-to-noise behavior in this sector means that interaction parameters of higher-partial waves should be accessible in the very near future, requiring 10X to 100X teraflop resources. Probing the three-nucleon force should coincide with measuring the triton with adequate precision—something that is expected to take 10X to 100X petaflop resources. Alpha particle precision measurements will take full exascale resources, and only at this scale can investigations away from the isospin limit be made. An understanding of isospin breaking forces, as well as non-leptonic parity violating nuclear forces, will require exascale resources and beyond.

These rough estimates are made using current experience and knowledge about lattice calculations. It is highly probable that disruptive technologies and algorithms will accelerate the timescale for achieving these goals.

## 6. Conclusion

High-performance computing is bringing nuclear physics into a new era where predictive capability will become the norm. In this process, answers to longstanding questions in fundamental physics will be attainable, and the connection between different subfields of nuclear physics will become stronger. Nowhere is this more realizable than in the area of nuclear forces, where high-performance computing is now allowing aspects of hadronic interactions to be ascertained from true *ab initio*, first principles LQCD calculations. The impact of these calculations will be far reaching, affecting the fields of nuclear structure and nuclear astrophysics, for example.

In these proceedings we described how future LQCD calculations will be used to extract hadronic interaction parameters and outlined a method for analyzing non-perturbative three-body systems that utilize box boundary conditions. We give estimates on computational resources needed to obtain important milestones. As we argued in these proceedings, LQCD promises to be calculational tool for nuclear physics of unprecedented power and scope. High-performance computing will make this promise come true.

## Acknowledgments

We thank members of NPLQCD for their inciteful critiques of this manuscript. Luu thanks M. Hruška for useful discussions. Walker-Loud was supported under OJI Grant DE-FG02-07ER41527. Luu performed this work under the auspices of the U.S. Department of Energy by Lawrence Livermore National Laboratory under Contract DE-AC52-07NA27344.

## References

- [1] Maiani L and Testa M 1990 *Phys. Lett.* **B245** 585–590
- [2] Huang K and Yang C N 1957 *Phys. Rev.* **105** 767–775
- [3] Luscher M 1986 *Commun. Math. Phys.* **105** 153–188
- [4] Luscher M 1991 *Nucl. Phys.* **B354** 531–578
- [5] Ishii N, Aoki S and Hatsuda T 2007 *Phys. Rev. Lett.* **99** 022001 (*Preprint nucl-th/0611096*)
- [6] Nemura H, Ishii N, Aoki S and Hatsuda T 2009 *Phys. Lett.* **B673** 136–141 (*Preprint 0806.1094*)
- [7] Detmold W, Orginos K and Savage M J 2007 *Phys. Rev.* **D76** 114503 (*Preprint hep-lat/0703009*)
- [8] Beane S R, Orginos K and Savage M J 2008 *Int. J. Mod. Phys.* **E17** 1157–1218 (*Preprint 0805.4629*)
- [9] Beane S R 2008 (*Preprint 0812.1236*)
- [10] Beane S R, Bedaque P F, Parreno A and Savage M J 2004 *Phys. Lett.* **B585** 106–114 (*Preprint hep-lat/0312004*)
- [11] Beane S R, Bedaque P F, Orginos K and Savage M J 2006 *Phys. Rev. Lett.* **97** 012001 (*Preprint hep-lat/0602010*)
- [12] Weinberg S 1966 *Phys. Rev. Lett.* **17** 616–621
- [13] Gasser J and Leutwyler H 1984 *Ann. Phys.* **158** 142
- [14] Beane S R, Bedaque P F, Orginos K and Savage M J (NPLQCD) 2006 *Phys. Rev.* **D73** 054503 (*Preprint hep-lat/0506013*)
- [15] Kaplan D B 1992 *Phys. Lett.* **B288** 342–347 (*Preprint hep-lat/9206013*)
- [16] Shamir Y 1993 *Nucl. Phys.* **B406** 90–106 (*Preprint hep-lat/9303005*)
- [17] Furman V and Shamir Y 1995 *Nucl. Phys.* **B439** 54–78 (*Preprint hep-lat/9405004*)
- [18] Orginos K and Toussaint D (MILC) 1999 *Phys. Rev.* **D59** 014501 (*Preprint hep-lat/9805009*)
- [19] Orginos K, Toussaint D and Sugar R L (MILC) 1999 *Phys. Rev.* **D60** 054503 (*Preprint hep-lat/9903032*)
- [20] Bernard C W *et al.* 2001 *Phys. Rev.* **D64** 054506 (*Preprint hep-lat/0104002*)
- [21] Bar O, Bernard C, Rupak G and Shores N 2005 *Phys. Rev.* **D72** 054502 (*Preprint hep-lat/0503009*)
- [22] Chen J W, O’Connell D, Van de Water R S and Walker-Loud A 2006 *Phys. Rev.* **D73** 074510 (*Preprint hep-lat/0510024*)
- [23] Bedaque P F, Sato I and Walker-Loud A 2006 *Phys. Rev.* **D73** 074501 (*Preprint hep-lat/0601033*)
- [24] Chen J W, O’Connell D and Walker-Loud A 2007 *Phys. Rev.* **D75** 054501 (*Preprint hep-lat/0611003*)
- [25] Orginos K and Walker-Loud A 2008 *Phys. Rev.* **D77** 094505 (*Preprint 0705.0572*)
- [26] Chen J W, O’Connell D and Walker-Loud A 2009 *JHEP* **04** 090 (*Preprint 0706.0035*)
- [27] Chen J W, Golterman M, O’Connell D and Walker-Loud A 2009 (*Preprint 0905.2566*)
- [28] Beane S R *et al.* 2008 *Phys. Rev.* **D77** 014505 (*Preprint 0706.3026*)

- [29] Colangelo G, Gasser J and Leutwyler H 2001 *Nucl. Phys.* **B603** 125–179 (*Preprint hep-ph/0103088*)
- [30] Leutwyler H 2008 (*Preprint 0808.2825*)
- [31] Beane S R *et al.* 2006 *Phys. Rev.* **D74** 114503 (*Preprint hep-lat/0607036*)
- [32] Beane S R *et al.* (NPLQCD) 2008 *Phys. Rev.* **D77** 094507 (*Preprint 0709.1169*)
- [33] Beane S R, Bedaque P F, Orginos K and Savage M J 2007 *Phys. Rev.* **D75** 094501 (*Preprint hep-lat/0606023*)
- [34] Beane S R, Detmold W and Savage M J 2007 *Phys. Rev.* **D76** 074507 (*Preprint 0707.1670*)
- [35] Detmold W and Savage M J 2008 *Phys. Rev.* **D77** 057502 (*Preprint 0801.0763*)
- [36] Beane S R *et al.* 2008 *Phys. Rev. Lett.* **100** 082004 (*Preprint 0710.1827*)
- [37] Detmold W *et al.* 2008 *Phys. Rev.* **D78** 014507 (*Preprint 0803.2728*)
- [38] Detmold W, Orginos K, Savage M J and Walker-Loud A 2008 *Phys. Rev.* **D78** 054514 (*Preprint 0807.1856*)
- [39] Beane S R *et al.* 2009 (*Preprint 0905.0466*)
- [40] Beane S R *et al.* 2009 (*Preprint 0903.2990*)
- [41] Johnson R C 1982 *Phys. Lett.* **B114** 147
- [42] Luu T 2008 (*Preprint 0810.2331*)
- [43] Moore D C and Fleming G T 2006 *Phys. Rev.* **D73** 014504 (*Preprint hep-lat/0507018*)
- [44] Gottlieb S A and Rummukainen K 1996 *Nucl. Phys. Proc. Suppl.* **47** 819–822 (*Preprint hep-lat/9509088*)
- [45] Pricoupenko L and Castin Y 2007 *Journ. Phys. A* **40** 12863 (*Preprint 0705.1502*)
- [46] Kreuzer S and Hammer H W 2009 *Phys. Lett.* **B673** 260–263 (*Preprint 0811.0159*)
- [47] Luu T C, Bogner S, Haxton W C and Navratil P 2004 *Phys. Rev.* **C70** 014316 (*Preprint nucl-th/0404028*)
- [48] Luu T and Schwenk A 2007 *Phys. Rev. Lett.* **98** 103202 (*Preprint cond-mat/0606069*)